Atomic Fluorine Anion Storage Emission Material C12A7-F^- and Etching of Si and SiO_2 by Atomic Fluorine Anions

Chongfu Song,[†] Jianqiu Sun,[†] Songbai Qiu,[†] Lixia Yuan,[†] Jing Tu,[†] Youshifumi Torimoto,[‡] Masayoshi Sadakata,[§] and Quanxin Li*,[†]

Department of Chemical Physics, Lab of Biomass Clean Energy, University of Science and Technology of China, Hefei, Anhui, 230026, P. R. China, Oxy Japan Corporation, 7 Floor, Miya Building, 4-3-4, Kojimachi, Chiyoda-ku, Tokyo 102-0083, Japan, and Department of Environmental Chemical Engineering, Kogakuin University, 2665-1, Nakano-machi Hachioji-shi, Tokyo 192-0015, Japan

Received August 4, 2007. Revised Manuscript Received February 20, 2008

The present study provides a novel approach to produce pure and stable atomic fluorine anions (F^-) in the gas phase by using the F^- storage emission material of $[Ca_{24}Al_{28}O_{64}]^{4+}\cdot(O^{2-})_{0.35}(F^-)_{3.30}$ (abbreviated as C12A7-F^-), synthesized by the solid-state reaction of CaF_2, $CaCO_3$, and γ-Al_2O_3. The anionic species stored in the C12A7-F^- material were dominated by the F^- anions, about $(1.9 \pm 0.3) \times 10^{21}$ cm^{-3}, accompanied by a small amount of O^{2-}, O^-, and O_2^-, via ion chromatography and electron paramagnetic resonance measurements, which corroborates that the anionic species emitted from the C12A7-F^- surface were dominated by the F^- anions (about 90%) together with a small amount of the O^- anions and electrons, identified by a time-of-flight mass spectroscopy. The absolute emission current density of F^- was sensitive to the surface temperature and extraction field, reaching about 16.7 ± 0.8 $\mu A/cm^2$ at 800 °C and 1200 V/cm. A pure and stable atomic fluorine anion beam was developed by using an electrochemistry implantation method. Particularly, the atomic fluorine anions were found to be useful for the etching of Si and SiO_2, evaluated by the morphological alterations via a field emission scanning electron microscope, and the surface composition's changes using X-ray photoelectron spectroscopy.

1. Introduction

Atomic fluorine anion (F^-) is a monovalent anion (or monovalent negative ion) through the attachment of an electron to atomic fluorine. As one of the important chemical intermediates, atomic fluorine anion is potentially useful in many fields such as semiconductor etching, filming, material modifications, and so forth.[1–7] Because anions have negative polarity and low electron affinity, it has been found that anion implantation or deposition into insulated material surfaces is more suitable than using positive implantation because of negligible "surface charging-up" in the former.[1,2,8] Halogen anions have also been used as an alternative to positive ions for ion fusion drivers in inertial confinement fusion, because electron accumulation would be prevented.[9]

The conventional method to form anions is through the attachment of a free low-energy electron to atom or through anion molecule reactions, appearing in processes such as plasma, electron impact, laser irradiation, and so forth. Anions generated in these processes, in general, are accompanied by the formation of manifold species and complicated. Recently, we developed a new approach to selectively generate anions of O^-,[10–13] OH^-,[14,15] and H^-[16,17] via the synthesized anionic storage emission materials. For example, the microporous material of C12A7-O^- can store and emit O^-, prepared by the solid-state reaction of $CaCO_3$ and γ-Al_2O_3 in the dry oxygen environment.[10–13,18] The

* To whom correspondence should be addressed. Telephone: +86-551-3601118. Fax: +86-551-3606689. E-mail: liqx@ustc.edu.cn.
[†] University of Science and Technology of China.
[‡] Oxy Japan Corporation.
[§] Kogakuin University.

(1) Shibayama, T.; Shindo, H.; Horiike, Y. *Plasma Sources Sci. Technol.* **1996**, *5*, 254.
(2) Shindo, H.; Sawa, Y.; Horiike, Y. *Jpn. J. Appl. Phys.* **1995**, *34*, L925.
(3) Ishikawa, J.; Tsuji, H.; Shibutani, K.; Ikai, H.; Gotoh, Y. *12th Int. Conf. Ion Implant. Technol. Proc.* **1998**, *2*, 716.
(4) Lau, W. M.; Bello, I.; Sayer, M.; Zou, L. *Appl. Phys. Lett.* **1994**, *64*, 300.
(5) Rauthan, C. M. S.; Virdi, G. S.; Pathak, B. C.; Karhigeyan, A. *J. Appl. Phys.* **1998**, *83*, 3668.
(6) Hanamoto, K.; Sasaki, M.; Miyashita, T.; Kido, Y.; Nakayama, Y.; Kawamoto, Y.; Fujiwara, M.; Kaigawa, R. *Nucl. Instrum. Methods Phys. Res., Sect. B* **1997**, *129*, 228.
(7) Ishikawa, J. *Rev. Sci. Instrum.* **1996**, *67*, 1410.
(8) Booth, J. P.; Corr, C. S.; Curley, G. A.; Jolly, J.; Guillon, J.; Földes, T. *Appl. Phys. Lett.* **2006**, *88*, 151502.
(9) Ishikawa, J. *Rev. Sci. Instrum.* **2000**, *71*, 1036.
(10) Li, Q. X.; Torimoto, Y.; Sadakata, M. Patent WO/2005/115913, 2005.
(11) Li, Q. X.; Torimoto, Y.; Sadakata, M. Japan Patent JP2004−160374, 2004.
(12) Li, Q. X.; Hayashi, K.; Nishioka, M.; Kashiwagi, H.; Hirano, M.; Torimoto, Y.; Hosono, H.; Sadakata, M. *Appl. Phys. Lett.* **2002**, *80*, 4259.
(13) Li, Q. X.; Hosono, H.; Hirano, M.; Hayashi, K.; Nishioka, M.; Kashiwagi, H.; Torimoto, Y.; Sadakata, M. *Surf. Sci.* **2003**, *527*, 100.
(14) Li, J.; Huang, F.; Wang, L.; Yu, S. Q.; Torimoto, Y.; Sadakata, M.; Li, Q. X. *Chem. Mater.* **2005**, *17*, 2771.
(15) Li, J.; Huang, F.; Wang, L.; Wang, Z. X.; Yu, S. Q.; Torimoto, Y.; Sadakata, M.; Li, Q. X. *J. Phys. Chem. B* **2005**, *109*, 14599.
(16) Huang, F.; Li, J.; Xian, H.; Tu, J.; Sun, J. Q.; Yu, S. Q.; Li, Q. X.; Torimoto, Y.; Sadakata, M. *Appl. Phys. Lett.* **2005**, *86*, 114101.
(17) Huang, F.; Li, J.; Wang, L.; Dong, T.; Tu, J.; Torimoto, Y.; Sadakata, M.; Li, Q. X. *J. Phys. Chem. B* **2005**, *109*, 12032.
(18) Hayashi, K.; Hirano, M.; Matsuishi, S.; Hosono, H. *J. Am. Chem. Soc.* **2002**, *124*, 738.

10.1021/cm702192j CCC: $40.75 © 2008 American Chemical Society
Published on Web 04/30/2008

structure of C12A7-O^- is characterized by a positive charged lattice framework $[Ca_{24}Al_{28}O_{64}]^{4+}$ including 12 subnanometer-sized cages with a free space of about 0.4 nm in diameter.[18,19] The storage features of O^- in the cage of C12A7-O^- have been investigated by the electron paramagnetic resonance (EPR) method.[18] On the other hand, the O^- anions stored in C12A7-O^- can be emitted into the gas phase by heating the material.[10–13] The emitted species from the C12A7-O^- surface were dominated by O^- (about 90%). More recently, we also synthesized various derivatives such as C12A7-OH^-[14,15] and C12A7-H^-[16,17] and found that these materials or the modified ones would be potentially used in a one-step synthesis of phenol from benzene,[20] the reduction of NO,[21] a fast microorganisms' inactivation,[22,23] and the dissociation and oxidation of oxygenated organic compounds.[24–26] In 2003, Hosono's group first synthesized a unique inorganic electride by exchanging free oxygen ions in the C12A7 cages with electrons.[27] The synthesized material, named C12A7:e^-, is the first room-temperature-stable electride and exhibits unique physical properties that can be used as excellent electronic conductors and electrides.[27–31]

As one of the derivatives of C12A7, the material of $Ca_{24}Al_{28}O_{64}F_4$ (or named $C_{11}A_7 \cdot CaF_2$) was first prepared by Jeevaratnam et al., who cosintered $C_{12}A_7$ with CaF_2 at 900−1300 °C and reported a lattice constant of 11.964 Å.[32] Its crystal structure was further revealed by Williams,[33–35] Yu et al.,[36] and Sango.[37] The material of $Ca_{24}Al_{28}O_{64}F_4$, belonging to the $I\bar{4}3d$ space group, possesses a body-centered cubic structure with a lattice constant in the range of 11.964−11.981 Å.[32–37] This material also has a typical positively charged framework of C12A7 with a unit cell content of $Ca_{24}Al_{28}O_{64}F_4$. Further X-ray diffraction (XRD) analysis indicates that its structure is disordered in that there are two sites, 0.50 Å apart, which may be occupied by calcium atoms, and the 12-fold sites used by fluorine atoms are only partially occupied.[35] On the other hand, because it plays an important role in the setting and hardening of fluoride-bearing cement, $C_{11}A_7 \cdot CaF_2$ has attracted much attention recently.[38–41]

The present work aims to (1) synthesize the F^- storage emission material being able to selectively store and emit the F^- anions, (2) study its storage and emission features, (3) develop a pure and stable F^- beam, and (4) provide a flexible and environmentally friendly method for the semiconductor etching or surface modification via atomic fluorine anions. The F^- storage emission material of C12A7-F^- was synthesized by the solid-state reaction of CaF_2, $CaCO_3$, and γ-Al_2O_3. We investigated the characteristics of C12A7-F^- and its storage and emission features by using XRD, EPR, and ion chromatography (IC). Particularly, the pure and stable F^- beam developed via the material would be potentially useful for semiconductor etching and surface modification.

2. Experimental Section

2.1. Sample Preparation. The storage emission material of C12A7-F^- was synthesized by the solid-state reaction of CaF_2, $CaCO_3$, and γ-Al_2O_3. Three powders of CaF_2, $CaCO_3$, and γ-Al_2O_3 with average particle diameter of 20−30 μm were mixed and grained at a molar ratio of $CaF_2/CaCO_3/\gamma$-Al_2O_3 = 1:11:7. The powder mixture was pressed to a slice with a diameter of 15 mm and a thickness of 1 mm by a pressure of 150−200 kg/cm^2. The slice samples were temperature-programmed to 1350 °C with heating rate of 15 °C/min and sintered at 1350 °C for 8 h under flowing dry Ar atmosphere. Then, the sample was annealed at 780 °C under a flowing F_2/Ar mixture (F_2/Ar = 5:95) atmosphere for 10 h. The flow rate of Ar/F_2 mixture was 100 mL/min. Finally, the sintered samples were naturally cooled to room temperature.

For the materials etching experiments, SiO_2 nanoballs (average diameter: 300 ± 100 nm) and Si wafers were tested. The preparation of the SiO_2 nanoballs has been described previously.[42] Briefly, tetraethyl orthosilicate (2.0 mL; 20%) and $NH_3 \cdot H_2O$ (5.0 mL; 25%) were dripped into the mixture of anhydrous ethanol (40.0 mL) and deionized water (3.0 mL). The solution was stirred for 8 h at room temperature. The SiO_2 nanoballs formed were centrifuged and washed with ethanol as well as water for 3−5 cycles, then dispersed into alcohol. Finally, the SiO_2 nanoballs were loaded on a clean quartz plate (or Au plate) by placing several drops of SiO_2 nanoball-dispersed alcohol. For Si wafer etching, p-type Si(100) wafers (impedance: 50 Ω·cm, thickness: 1 mm), donated by Shin-Etsu Chemical Co. Ltd., Tokyo, were used. Before being etched, the Si wafers were cleaned with acetone in an ultrasonic bath, followed by being cleaned with ethanol and washed with copious deionized water 3−5 times.

2.2. Anion Emission Experiments. The emitted anions from C12A7-F^- were mass-analyzed by a time-of-flight (TOF) mass spectrometer. The detailed conditions in this contribution are virtually the same as those in previous work.[12,13,43] In brief, the apparatus essentially consisted of an anion emission chamber and a TOF mass spectrometry. The emission material was supported

(19) Bartl, H. B.; Scheller, T. *Neues Jahrb. Mineral. Monatsh.* **1970**, *35*, 547.
(20) Dong, T.; Li, J.; Huang, F.; Wang, L.; Tu, J.; Torimoto, Y.; Sadakata, M.; Li, Q. X. *Chem. Commun.* **2005**, *21*, 2724.
(21) Gao, A. M.; Zhu, X. F.; Wang, H. J.; Tu, J.; Lin, P. Y.; Torimoto, Y.; Sadakata, M.; Li, Q. X. *J. Phys. Chem. B* **2006**, *110*, 11854.
(22) Wang, L.; Gong, L.; Zhao, E.; Yu, Z.; Torimoto, Y.; Sadakata, M.; Li, Q. X. *Lett. Appl. Microbiol.* **2007**, *45*, 200.
(23) Li, L. C.; Wang, L.; Yu, Z.; Lv, X. Z.; Li, Q. X. *Plasma Sci. Technol.* **2007**, *9*, 119.
(24) Wang, Z. X.; Pan, Y.; Dong, T.; Zhu, X. F.; Kan, T.; Yuan, L. X.; Torimoto, Y.; Sadakata, M.; Li, Q. X. *Appl. Catal., A* **2007**, *320*, 24.
(25) Dong, T.; Wang, Z. X.; Yuan, L. X.; Torimoto, Y.; Sadakata, M.; Li, Q. X. *Catal. Lett.* **2007**, *119*, 29.
(26) Wang, Z. X.; Dong, T.; Yuan, L. X.; Kan, T.; Zhu, X. F.; Torimoto, Y.; Sadakata, M.; Li, Q. X. *Energy Fuels* **2007**, *21*, 2421.
(27) Matsuishi, S.; Toda, Y.; Miyakawa, M.; Hayashi, K.; Kamiya, T.; Hirano, M.; Tanaka, I.; Hosono, H. *Science* **2003**, *301*, 626.
(28) Toda, Y.; Matsuishi, S.; Hayashi, K.; Ueda, K.; Kamiya, T.; Hirano, M.; Hosono, H. *Adv. Mater.* **2004**, *16*, 685.
(29) Kamiya, T.; Aiba, S.; Miyakawa, M.; Nomura, K.; Matsuishi, S.; Hayashi, K.; Ueda, K.; Hirano, M.; Hosono, H. *Chem. Mater.* **2005**, *17*, 6311.
(30) Miyakawa, M.; Kim, S. W.; Hirano, M.; Kohama, Y; Kawaji, H.; Atake, T.; Ikegami, H.; Kono, K.; Hosono, H. *J. Am. Chem. Soc.* **2007**, *129*, 7270.
(31) Kim, S. W.; Matsuishi, S.; Nomura, T.; Kubota, Y.; Takata, M.; Hayashi, K.; Kamiya, T.; Hirano, M.; Hosono, H. *Nano Lett.* **2007**, *7*, 1138.
(32) Jeevaratnam, J.; Glasher, F. P.; Glasser, L. S. *J. Am. Ceram. Soc.* **1964**, *47*, 105.
(33) Williams, P. P. *Proc. 5th Int. Symp. Chem. Cem.* **1968**, *I*, 366.
(34) Williams, P. P. *J. Am. Ceram. Soc.* **1968**, *51*, 531.
(35) Williams, P. P. *Acta Crystallogr., Sect. B* **1973**, *29*, 1550.
(36) Yu, Q. J.; Shuichi, S.; Feng, X. J.; Mi, J. X. *Cem. Concr. Res.* **1997**, *27*, l439.
(37) Sango, H. *J. Eur. Ceram. Soc.* **2006**, *26*, 803.
(38) Odler, I.; Abdul-Maula, S. *J. Am. Ceram. Soc.* **1980**, *63*, 654.
(39) Wang, S. B.; Ding, W. C. *J. Chin. Ceram. Soc.* **1988**, *16*, 305.
(40) Sango, H.; Miyakawa, T.; Kasai, J. *J. Chem. Soc. Jpn.* **1990**, *3*, 305.
(41) Park, C. K. *Cem. Concr. Res.* **1998**, *28*, 1357.
(42) Wang, L. Y.; Li, Y. D. *Small* **2007**, *3*, 1218.

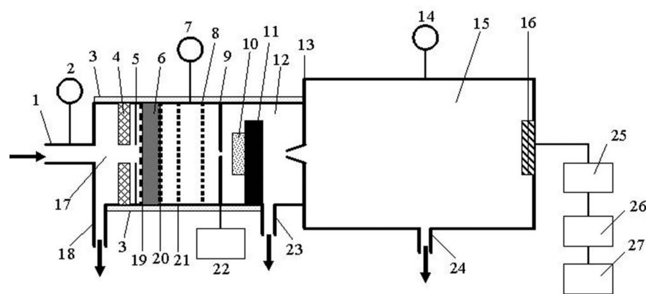

Figure 1. Etching system by atomic fluorine anion beam. 1: halogen gas inlet port; 2: thermocouple gauge; 3: cooling-water system; 4: heater; 5: quartz plate; 6: anion storage emission material; 7: ionization gauge; 8: anion energy adjusted electrode; 9: Faraday plate (or shutter); 10: etched sample; 11: etched sample holder; 12: anion emission chamber; 13: vacuum skimmer; 14: ionization gauge; 15: anion free flight section; 16: tandem microchannel plates; 17: anion implantation chamber; 18: mechanism pump inlet port; 19: electron supply electrode; 20: anion extraction electrode; 21: ground electrode; 22: amperometer; 23: molecular pump inlet port; 24: molecular pump inlet port; 25: amplifier; 26: digital oscilloscope; 27: computer-controlled counter system.

by a quartz plate mounted in the emission chamber. The emission material was heated by a quartz-sealed Fe−Cr alloy filament to avoid any influence of electron emission from the filament. The emitted anions from the material surface were extracted by an extraction electrode. Total emission current was collected by a Faraday plate and detected by a Keithley model 6485 amperometer. A small amount of the anions passed through a pinhole of 1 mm in the Faraday plate, which allowed a simultaneous analysis of the emitted anion distribution by a TOF mass spectrometry. All tests were repeated three times. The difference for each replicate generally ranged from 0 to 25%. The results given were average values.

2.3. Materials Etching Experiments. As illustrated in Figure 1, the etching system by the atomic fluorine anion beam mainly consists of a stable anion source of F$^-$ using the C12A7-F$^-$ material, an anion extraction electrode, an ion-energy adjusted electrode, a shutter, and an etched sample holder. A sustainable and stable F$^-$ beam is guaranteed by an electrochemistry implantation method, as discussed in section 3.2. Before the etching operation, the F$^-$ intensity of the source and that on the holder position were calibrated. The extracted F$^-$ anions passed through the ion-energy adjusted electrode and shutter. Then, the atomic fluorine anion beam (intensity: 0−17 μA/cm^2; energy: 0−1600 eV) was exposed onto the etched material surface mounted on the sample holder. On running the etching for the Si wafer, part of the Si surface was masked with a quartz slice for comparison. The gas pressure in the etching region in operation was maintained to be less than 2×10^{-3} Pa. The etching rate was estimated from the etched depth via the field emission scanning electron microscope (FESEM) measurements and etching time for each sample under a given etching condition.

2.4. Material Characterization. XRD measurements were carried out to investigate the structure of C12A7-F$^-$. The synthesized C12A7-F$^-$ samples were crushed into an average diameter of 20−30 μm. Powder XRD patterns were recorded on an X'pert Pro Philips diffractometer with a Ni-filtered Cu Kα1 source (λ = 1.540598 Å). The measurement conditions were in the 2θ range of 10−80°, step counting time of 5 s, and step size of 0.017° at 298 K. The measurement of the unit cell value was made from diffractometer traces using Si as the internal standard.

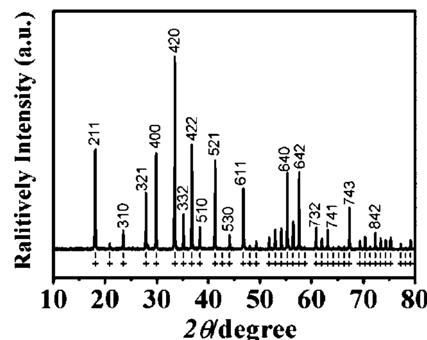

Figure 2. XRD pattern of a C12A7-F$^-$ sample. The tick marks indicate the reflection positions of the C12A7-F$^-$ sample, and the plus signs indicate the positions of the diffraction peaks given in the PDF-74−2116 card.

EPR measurements were performed to investigate the anionic species in the C12A7-F$^-$ bulk. EPR experiments were conducted at ~9.1 GHz (X-band) using a JES-FA200 spectrometer at 77 K. Spin concentrations were determined from the second integral of the spectrum using $CuSO_4 \cdot 5H_2O$ as a standard with an error of about 20%. The absolute F$^-$ concentration in the C12A7-F$^-$ (after dissolving in the deionized water) was analyzed by using an IC (DX-120, Dionex Co.) method and calibrated with a standard of 4.0×10^{-4} mol/L NaF solution.

The surface elements were analyzed by X-ray photoelectron spectroscopy (XPS). The XPS measurements were performed on an ESCALAB-250 (Thermo-VG Scientific) spectrometer with Al Kα (1486.6 eV) irradiation source. The background pressure of the analytical chamber was 1.0×10^{-9} Torr. The analyzed surface was 2 mm in diameter, and the takeoff angle of photoelectrons was 90° with respect to sample surface. The normalized XPS intensities, which are proportional to the concentrations of the corresponding elements in the surface layer, were determined as the integrated peak area divided by their corresponding sensitivity factor. The C(1*s*) peak at 284.6 eV was used as a calibration standard for determining the peaks' positions and the elemental concentrations.

To examine the morphological alteration, the Si and SiO_2 samples for the pristine and etched ones were coated with a gold layer about 3 nm (SCD 050 Sputter Coater, BAL-TEC) and then observed using a FEI Sirion-200 FESEM.

3. Results and Discussion

3.1. Structure and Characteristics of C12A7-F$^-$. The XRD measurement was carried out to investigate the structure of C12A7-F$^-$. Figure 1 shows the XRD pattern of the C12A7-F$^-$ material prepared. For comparison, the positions of the diffraction peak given in PDF-74−2116 (International Centre for Diffraction Data, 2003)[35] was also labeled in Figure 2. By comparing the measured peak positions and intensities of the XRD pattern with the standard data in the PDF-74−2116 card, we found that the X-ray diffraction structure for the present C12A7-F$^-$ material is completely in accord with that of $C11A7 \cdot CaF_2$ (with a unit cell content of $Ca_{24}Al_{28}O_{64}F_4$), belonging to the $I\bar{4}3d$ space group. No other phases such as $Ca_5Al_6O_{14}$ (C5A3), $Ca_3Al_2O_6$ (C3A), and $CaAl_2O_4$ (CA)[44–47] were observed. Thus, the

(43) Li, Q. X.; Hayashi, K.; Nishioka, M.; Kashiwagi, H.; Hirano, M.; Torimoto, Y.; Hosono, H.; Sadakata, M. *Jpn. J. Appl. Phys.* **2002**, *41*, L530.
(44) Vincent, M. G.; Jeffery, J. W. *Acta Crystallogr., Sect. B* **1978**, *34*, 1422.
(45) Mondal, P.; Jeffery, J. W. *Acta Crystallogr., Sect. B* **1975**, *31*, 689.
(46) Zhmoidin, G. I.; Chatterjee, A. K. *Cem. Concr. Res.* **1984**, *14*, 386.

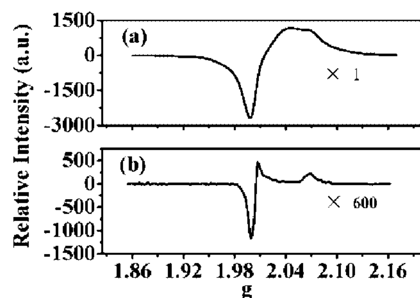

Figure 3. EPR spectra for (a) C12A7-O$^-$ and (b) C12A7-F$^-$. "×1" and "×600" stand for the amplified time of the EPR signal.

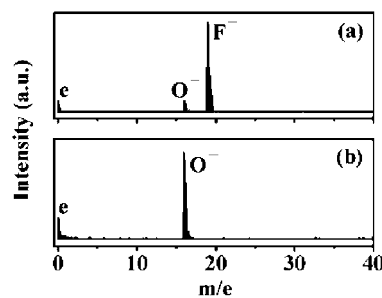

Figure 4. Typical TOF mass spectra measured at 750 °C and 1000 V/cm for (a) C12A7-F$^-$ sample and (b) C12A7-O$^-$ sample. The emission purity of F$^-$ from C12A7-F$^-$, described by the intensity ratio of $I(F^-)/[I(e^-) + I(O^-) + I(F^-)]$, is about 0.9.

impurity phase in the C12A7-F$^-$ material prepared is negligible beside the $Ca_{24}Al_{28}O_{64}F_4$ phase. The unit cell value derived from 20 stronger diffraction peaks is about 11.969 ± 0.002 Å, which agrees very well with the previous reported data of 11.970 Å.[35]

EPR measurements were performed to investigate the anionic species in the C12A7-F$^-$ bulk, and the results were compared with those in C12A7-O$^-$. As shown in Figure 3a, the EPR spectra for C12A7-O$^-$ can be decomposed into two components, which were attributed to the anionic oxygen species of O$^-$ ($g_{xx} = g_{yy} = 2.043$ and $g_{zz} = 1.997$) and O_2^- ($g_{xx} = 2.001$, $g_{yy} = 2.010$, and $g_{zz} = 2.070$).[14,18,48–50] The spectral profile of C12A7-F$^-$ (Figure 3b), on the whole, is similar to that of C12A7-O$^-$. However, the spectral intensity for C12A7-F$^-$ is significantly weaker than that of C12A7-O$^-$. By simulating the EPR spectra and using $CuSO_4 \cdot 5H_2O$ as a spin concentrations standard, we can estimate the concentrations of the anionic oxygen species in the bulk. For C12A7-O$^-$, the concentrations of O$^-$ and O_2^- are nearly equal by simulating the measured EPR spectra, being about $(2.7 \pm 0.5) \times 10^{20}$ cm^{-3} and $(2.6 \pm 0.6) \times 10^{20}$ cm^{-3}, respectively. However, the total concentration of O$^-$ ($(5.8 \pm 1.5) \times 10^{16}$ cm^{-3}) and O_2^- ($(5.1 \pm 1.2) \times 10^{17}$ cm^{-3}) in C12A7-F$^-$ sharply decreased to 5.7×10^{17} cm^{-3}, which is only about 0.1% of that in C12A7-O$^-$. The EPR results show that, for the C12A7-F$^-$ material, nearly all of the O$^-$ and O_2^- anions translate to other anion species. The substituted species in the C12A7-F$^-$ cages should be attributed to the F$^-$ anions because of the desorbed species being almost F$^-$ anions (section 3.2). However, this EPR method cannot be used directly to measure the F$^-$ species in the C12A7-F$^-$ material because there is no unpaired electron for the F$^-$ anions. The absolute F$^-$ concentration in the C12A7-F$^-$ was further analyzed by using the IC method and calibrated with a standard solution of 4.0×10^{-4} mol/L NaF, giving an average value of $(1.9 \pm 0.3) \times 10^{21}$ cm^{-3}. On the other hand, the species of O^{2-} was about $(2.0 \pm 0.4) \times 10^{20}$ cm^{-3}in C12A7-F$^-$, which was estimated by the charge balance, total positive charge concentration (2.3×10^{21} cm^{-3}),[14,18,48–50] and all anionic species measured. Accordingly, the anionic species in the synthesized material were dominated by the F$^-$ anions, accompanied by small amounts of O^{2-}, O$^-$, and O_2^-, which also agrees with the distribution of the emitted anions via the TOF observations (section 3.2). The chemical formula of the present material could be approximately described as $[Ca_{24}Al_{28}O_{64}]^{4+} \cdot (O^{2-})_{0.35}(F^-)_{3.30}$ (abbreviated as C12A7-F$^-$). It is noticed that the F$^-$ number (n= 3.30) in the C12A7-F$^-$ material is lower than four, indicating incomplete translation from O^{2-} to F$^-$ during the preparation process of C12A7-F$^-$. This phenomenon was also observed in the preparation processes of other derivatives of C12A7, for example, C12A7-O$^-$ (n = 1.04,[18] 1.20,[14] 2.96 [49]), C12A7-H$^-$ (n = 0.43),[51] C12A7-OH$^-$ (n = 1.20),[14,15] and C12A7-e$^-$ (n = 0.05,[52] 3.26,[53] 3.48 [27]).

3.2. Anion Emission Properties of C12A7-F$^-$. The anions emitted from the C12A7-F$^-$ surface were identified by a TOF mass spectroscopy. As shown in Figure 4a, the anionic species emitted from the C12A7-F$^-$ material surface were dominated by the F$^-$ anions (about 90%) together with a small amount of O$^-$ anions (about 5%) and electron emission (about 5%) under a typical emission condition (at 750 °C with an extraction field of 1000 V/cm). In contrast, the desorbed species from the C12A7-O$^-$ surface were dominated by O$^-$ (~90%) together with a small amount of electrons (~10%) under the same condition (Figure 4b). The alteration of the anionic distribution emitted from the C12A7-F$^-$ indirectly demonstrates that F$^-$ anions should be the major anions stored in the cages of C12A7-F$^-$.

The absolute emission current density of F$^-$ was obtained on the basis of the calibration of the total emission current density with the anionic distribution detected by TOF mass spectra. Table 1 shows the absolute emission current density of F$^-$ emitted from the C12A7-F$^-$ material at different temperatures and extraction fields. The emission current density of F$^-$ strongly depends on the surface temperature and increases from 20 ± 10 nA/cm^2 to 16.7 ± 0.8 μA/cm^2 when the temperature rises from 520 to 800 °C at a fixed extraction field of 1200 V/cm. On the other hand, with the increase of extraction field from 200 to 1200 V/cm, the F$^-$ emission current density increases from 0.5 ± 0.1 to 16.6 ±

(47) Palacios, L.; De La Torre, Á. G.; Bruque, S.; Garcı´a-Muñoz, J. L.; Garcı´a-Granda, S.; Sheptyakov, D.; Aranda, M. A. G. *Inorg. Chem.* **2007**, *46*, 4167.
(48) Hosono, H.; Abe, Y. *Inorg. Chem.* **1987**, *26*, 1192.
(49) Hayashi, K.; Matsuishi, S.; Ueda, N.; Hirano, M.; Hosono, H. *Chem. Mater.* **2003**, *15*, 1851.
(50) Yang, S. W.; Kondo, J. N.; Hayashi, K.; Hirano, M.; Domen, K.; Hosono, H. *Chem. Mater.* **2004**, *16*, 104.
(51) Hayashi, K.; Matsuishi, S.; Kamiya, T.; Hirano, M.; Hosono, H. *Nature* **2002**, *419*, 462.
(52) Kim, S. W.; Toda, Y.; Hayashi, K.; Hirano, M.; Hosono, H. *Chem. Mater.* **2006**, *18*, 1938.
(53) Miyakawa, M.; Hirano, M.; Kamiya, T.; Hosono, H. *Appl. Phys. Lett.* **2007**, *90*, 182105.

Table 1. Absolute Emission Current Density of F$^-$ Emitted from the C12A7-F$^-$ Material at a Series of Temperatures and Extraction Fields

temperature (°C)	extraction field (V/cm)	emission current density (μA/cm^2)[a]
520	1200	0.02 ± 0.01[b]
550	1200	0.3 ± 0.1
600	1200	0.4 ± 0.2
650	1200	1.4 ± 0.2
700	1200	2.5 ± 0.3
750	1200	4.4 ± 0.6
780	1200	9.5 ± 0.5
800	1200	16.7 ± 0.8
800	200	0.5 ± 0.1
800	400	2.1 ± 0.5
800	600	3.9 ± 0.6
800	800	5.9 ± 0.7
800	1000	9.6 ± 0.6
800	1200	16.6 ± 0.8

[a] The absolute emission current density of F$^-$ was obtained on the basis of the calibration of the total emission current density with the anionic distribution detected by TOF mass spectra. [b] All values were the average ones tested from three C12A7-F$^-$ samples.

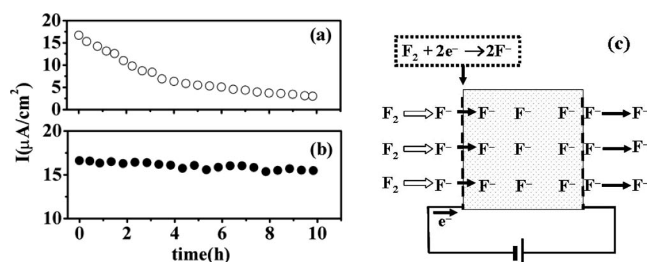

Figure 5. Emission densities of F$^-$ measured at 800 °C and 1200 V/cm as a function of operating time: (a) without implantation and (b) with implantation of F_2/Ar mixture gas (F_2/Ar = 1:9; pressure: ~2.0 Torr) and electrons on backside of the C12A7-F$^-$ sample (implantation voltage: −10 V). (c) Schematic setup shows the online implantation and emission of atomic fluorine anions, which continuously generated the consumed F$^-$ anions via the electrochemical catalytic reaction ($F_2 + 2e^- \rightarrow 2F^-$) on the backside of the C12A7-F$^-$ sample and migrated into the C12A7-F$^-$ material.

0.8 μA/cm^2 at 800 °C. With increasing temperature and/or extraction field, both the anion's diffusion and desorption processes would be enhanced,[12–17] leading to the increase of the F$^-$ emission at higher temperature or higher extraction field.

The stability of the F$^-$ emission from C12A7-F$^-$ was investigated as a function of emission duration. The emission intensity of F$^-$ gradually decreases with increasing operation time (Figure 5a). The intensity dropped to about 38% of the initial one after 4 h of emission at 800 °C and 1200 V/cm. The emission decay mainly caused by the concentration decrease of the F$^-$ anions which was stored in the C12A7-F$^-$ with increasing emission time. To obtain a sustainable and stable F$^-$ emission beam, we adopted a simple electrochemistry implantation method by supplying a fluorine/argon mixture gas (F_2/Ar = 1:9, ~2 Torr) and electrons (by applying a low negative direct current−voltage of −10 V) on the backside of the C12A7-F$^-$ material (Figure 5c), where F$^-$ (surface) was generated by the electrochemical catalytic reaction, F_2 (surface) + 2e$^-$ (surface) → 2F$^-$ (surface), and then migrated into the cage of the C12A7-F$^-$ by the field-enhanced thermal diffusion. The electrochemistry implantation method was also used for compensating the consumed O$^-$ from C12A7-O$^-$,[12,38] OH$^-$ from C12A7-OH$^-$,[14] and H$^-$ from C12A7-H$^-$.[16] As shown in Figure 5b, the emission current density of F$^-$ was almost stable within the tested operating duration (about 10 h) by the continuous electrochemistry implantation method mentioned above. This allows one to develop a relatively pure and stable atomic fluorine anion emission beam.

3.3. Etching of Materials Using the F$^-$ Anion Beam. The present work provides a method to produce a relatively pure (purity: 90%) and stable F$^-$ anion beam via the F$^-$ emission material of C12A7-F$^-$, which is useful for etching or surface modification for the semiconductor materials or other materials. Two types of materials, Si and SiO_2, were investigated for the etching tests. The etching performances mainly depend upon the F$^-$ current density, the F$^-$ ion energy, and etching time. For the SiO_2 samples etched by the F$^-$ anion beam (16.5 ± 0.8 μA/cm^2), the etching rates were about 3.3, 12.5, and 18.9 nm/min at the ion energies of 100, 800, and 1600 eV, respectively. Moreover, for the Si samples etched via the F$^-$ anion beam of 16.5 ± 0.8 μA/cm^2, the etching rates were about 6.7, 24.1, and 35.0 nm/min at 100, 800, and 1600 eV, respectively. The threshold energy of the etching was about 8 eV for the Si samples, which was less than that of the physical sputtering energy of 20 eV.[54] This means that the chemical sputtering may take place dominantly in the low- energy etching, where fluoridation of Si would decrease the threshold energy.

To examine the morphological alteration by the F$^-$ etching, the etched SiO_2 samples were investigated by the FESEM measurements. Figure 6 shows the FESEM images from (a) the pristine SiO_2 sample (SiO_2 nanoballs Φ: 300 ± 100 nm), (b) the etched SiO_2 sample via the F$^-$ anion beam (16.5 ± 0.8 μA/cm^2, 1600 eV) for 3 min, and (c) the etched SiO_2 sample via the F$^-$ anion beam (16.5 ± 0.8 μA/cm^2, 1600 eV) for 15 min. In contrast to the morphology of the pristine sample, obvious morphologic deformation was observed for the etched SiO_2 nanoballs for 3 min. The SiO_2 nanoballs were almost fragmented via the F$^-$ etching for 15 min. For the evaluation of the surface composition alterations by the F$^-$ etching, the etched SiO_2 surfaces were further investigated using the XPS measurements. Figure 7 shows the wide-scan XPS spectra of (a) the pristine SiO_2 sample, (b) the etched SiO_2 sample via the F$^-$ anion beam (16.5 ± 0.8 μA/cm^2, 1600 eV) for 3 min, and (c) the etched SiO_2 sample via the F$^-$ anion beam (16.5 ± 0.8 μA/cm^2, 1600 eV) for 15 min. For the pristine SiO_2 sample (Figure 7a), three strong peaks were observed in the range of 0−900 eV, which were assigned to the Si(2*p*) peak at 103.3 eV, the Si(2*s*) peak at 154.0 eV, and the O(1*s*) peak at 532.6 eV.[55] For the etched SiO_2 sample via the F$^-$ beam (16.5 ± 0.8 μA/cm^2, 1600 eV) (Figure 7b,c), however, three new peaks involving atomic fluorine, that is, F(1*s*) at 686.7 eV, F(2*s*) at 32.0 eV, and F(KLL) at 834.4 eV,[56] were observed. With increased etching time, the relative intensity of the F(1*s*) peak

(54) Barone, M. E.; Graves, D. B. *J. Appl. Phys.* **1995**, *77*, 1263.
(55) Zhu, X. P.; Yukawa, T.; Hirai, M.; Suematsu, H.; Jiang, W. H.; Yatsui, K.; Nishiyama, H.; Inoue, Y. *Appl. Surf. Sci.* **2006**, *252*, 5776.
(56) Hanamoto, K.; Yoshimoto, H.; Hosono, T.; Hirai, A.; Kido, Y.; Nakayama, Y.; Kaigawa, R. *Nucl. Instrum. Methods Phys. Res., Sect. B* **1998**, *140*, 124.

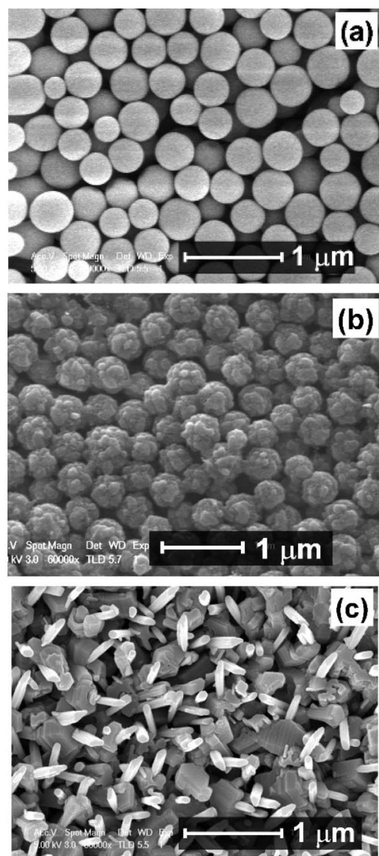

Figure 6. FESEM photographs of (a) the pristine SiO_2 sample (SiO_2 nanoballs Φ: 300 ± 100 nm), magnification: 80 000×; (b) the etched SiO_2 sample via the F^- anion beam (16.5 ± 0.8 $\mu A/cm^2$, 1600 eV) for 3 min, magnification: 60 000×; and (c) the etched SiO_2 sample via the F^- anion beam (16.5 ± 0.8 $\mu A/cm^2$, 1600 eV) for 15 min, magnification: 80 000×.

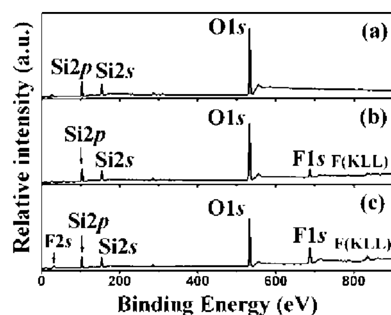

Figure 7. XPS wide-scan spectra of (a) the pristine SiO_2 sample, (b) the etched SiO_2 sample via the F^- anion beam (16.5 ± 0.8 $\mu A/cm^2$, 1600 eV) for 3 min, and (c) the etched SiO_2 sample via the F^- anion beam (16.5 ± 0.8 $\mu A/cm^2$, 1600 eV) for 15 min.

increased, accompanied by a simultaneous decrease of the intensities of Si(2*p*) as well as O(1*s*).

A more quantitative analysis of the composition variations before and after the etching was also completed. The relative content (atomic %) of silicon atoms (Si(2*p*)) measured on the pristine SiO_2 sample was about 30.7% and decreased to 29.3 and 28.1% for 3 and 15 min of etching via the F^- beam (16.5 ± 0.8 $\mu A/cm^2$, 1600 eV), respectively. The relative content of fluorine atoms (F(1*s*)) for the F^--etched samples was about 5.7 and 17.0% after the etching treatment for 3 and 15 min, and the atomic ratios of fluorine to silicon for

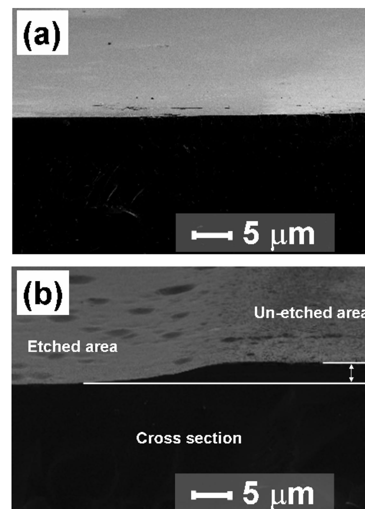

Figure 8. FESEM photographs of (a) the pristine Si wafer, magnification: 6000×; (b) the etched Si wafer via the F^- anion beam (16.5 ± 0.8 $\mu A/cm^2$, 1600 eV) for 1.5 h, magnification: 6000×. The arrow stands for the etched depth.

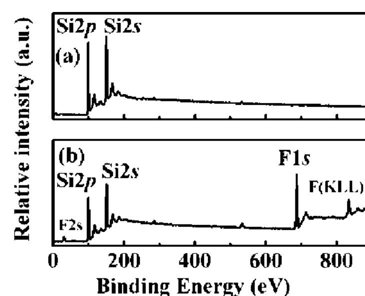

Figure 9. XPS wide-scan spectra of (a) the pristine Si wafer and (b) the Si wafer etched by the F^- anion beam (16.5 ± 0.8 $\mu A/cm^2$, 1600 eV) for 1.5 h.

the etched SiO_2 samples were about 0.19 and 0.61, respectively.

In addition, the etching behavior of the Si wafer via the F^- beam was also examined by FESEM and XPS measurements. Figure 8 presents the FESEM images of (a) the pristine Si wafer (the p-type Si(100) wafers, impedance: 50 Ω·cm, thickness: 1 mm) and (b) the etched one with the F^- beam (16.5 ± 0.8 $\mu A/cm^2$, 1600 eV) for 1.5 h. For the etched Si wafer, the FESEM image displays three different areas: the etched area (I), the unetched area (II), and the cross section (III). It was observed that an obvious etching layer of silicon (side step) with a depth of 2.8 μm formed after the F^- etching. Figure 9 shows the wide-scan XPS spectra from (a) the pristine Si wafer and (b) the etched one via the F^- beam (16.5 ± 0.8 $\mu A/cm^2$, 1600 eV) for 1.5 h. For the pristine Si wafer, only two peaks, Si(2*p*) at 98.8 eV and Si(2*s*) at 150.8 eV,[57] were observed in the range of 0−900 eV. For the etched Si wafer via the F^- beam (16.5 ± 0.8 $\mu A/cm^2$, 1600 eV) for 1.5 h, three new peaks involving atomic fluorine, that is, F(1*s*) at 685.6 eV, F(2*s*) at 31.0 eV, and F(KLL) at 833.7 eV,[56] appeared. In addition, it was also noticed that the relative intensities of the Si(2*p*) and Si(2*s*) peaks for the F^--etched Si wafer significantly decreased after

(57) Aygun, G.; Atanassova, E.; Kostov, K.; Turan, R. *J. Non-Cryst. Solids* **2006**, *352*, 3134.

the etching. On the basis of the quantitative composition analysis, the relative content of silicon atoms (Si(2*p*)) on the pristine Si wafer was about 95.0% and dropped to 65.0% after 1.5 h of etching (16.5 ± 0.8 μA/cm^2, 1600 eV). Simultaneously, the relative content of fluorine atoms measured on the etched Si surface increased by 29.0% (from 0 to 29.0%) for 1.5 h of etching. The atomic ratio of fluorine to silicon for the etched Siwafer surface was about 0.45. Thus, these results would suggest that the fluoridation of Si or SiO_2 occurred during the F^- etching process, leading to the morphological and compositional alterations on the etched surfaces. To elucidate further the etching's mechanism, the process needs further work (e.g., formation of chemical bond), and work toward this goal is in progress.

4. Conclusions

We have investigated a novel approach to produce pure and stable atomic fluorine anions (F^-) in the gas phase by using the F^- storage emission material of C12A7-F$^-$ ($[Ca_{24}Al_{28}O_{64}]^{4+} \cdot (O^{2-})_{0.35}(F^-)_{3.30}$) and Si and SiO_2 etching via atomic fluorine anions. The synthesized C12A7-F$^-$, having the cage structure, selectively stored atomic fluorine anions with concentration about $(1.9 \pm 0.3) \times 10^{21}$ cm^{-3}. The anionic species emitted from the C12A7-F$^-$ surface were dominated by the F^- anions (about 90%). The absolute emission current density of F^- reached about 16.7 ± 0.8 μA/cm^2 at 800 °C with an extraction field of 1200 V/cm. A pure and stable atomic fluorine anion beam was developed by using an electrochemistry implantation method for the C12A7-F$^-$ material. It was also revealed that the developed F^- beam was useful for materials etching of Si and SiO_2. Potentially, the F^- storage emission material and the formed F^- beams might also be extended to other fields such as material modifications, inertial confinement fusion, atmospheric chemistry, particle accelerators, as well as other areas.

Acknowledgment. We are grateful to the support of the General Program of the National Natural Science Foundation of China (No. 50772107), the National High Tech Research and Development Program (863 Program No. 2006AA05Z118), and the National Basic Research Program (973 Program No. 2007CB210206) of the Ministry of Science and Technology of China.

CM702192J